Rheokinetic of Polyurethane Crosslinking Time-Temperature-Transformation Diagram for Rotational Molding

S. Farzaneh, S. Riviere, A. Tcharkhtchi

PIMM, Arts et Métiers ParisTech (ENSAM)—UMR 8006 (CNRS), 151 Bd de l'Hôpital, 75013 Paris, France

ABSTRACT: In this work, the rheokinetic of polyurethane crosslinking was studied by different methods: differential scanning calorimetric (DSC), rheometry, and infrared spectrometry. The conversion ratio and the glass transition temperature were followed by time of reaction. The results of the isothermal and nonisothermal test were compared. The evolution of viscosity was measured at different frequencies. The intersection of these curves is considered as gel point. A simplified mechanism has been proposed for crosslinking reactions. Based on this mechanism, a kinetic model describing the evolution of reactive system was developed. This model then was compared with the results of experiments performed by infrared spectrometry. The time-temperature-transformation diagram was established showing the evolution of physical state change of the reactive system. This diagram may be used to evaluate the zone of rotomoldability of the reactive polyurethane.

Key words: reactive processing; polyurethane; crosslinking; vitrification; gelation; TTT diagram; rotational molding

INTRODUCTION

Reactive rotational molding is an alternative processing method to the use of thermoplastic powders with several advantages.[1–3] The process, in general, can be carried out at lower temperatures compared to the rotational molding of the thermoplastic powders. For certain polyurethans and polyepoxy, the rotational molding is carried out at room temperature. The time of the cycle depends on the rate of reactions between the components. It can be very short such as a few minutes. The process is very economical, because the chemical reaction for synthesis of polymer and the transformation of polymer to the product are carried out in the same operation. Besides, this process is the only way for rotational molding of thermosets and rubbers.

In reactive rotational molding, the viscosity is the main parameter during evolution of reactive system.

Figure 1 shows the evolution of viscosity, as the process starts, the viscosity of the system decreases under the effect of the heating until reaches a minimal value, η_{min}.

From this point, the crosslinking reaction prevails and the viscosity starts to increase but the fluidity is too high and the liquid cannot yet be rotomolded. To rotomold the viscosity should reach at least to a specific value, $(\eta_r)_{min}$. By increasing of the molecular weight, the mobility of the system decreases and the viscosity increases in a very fast way to reach a upper limit, $(\eta_r)_{max}$. From this limit, the rotomolding is practically impossible. Viscosity becomes too high and the material is relatively motionless.

Simplified model polyurethane synthesis

In this study, the reactive system is polyurethane.[4,5] Polyurethanes are polymers with a vast range of formulations. They have different hardness, stiffness, and densities, and thus, polyurethanes may appear in the form of low-density flexible foams, low-density rigid foams, soft-solid rubbers, or hard-solid plastics. Because of their versatility, they have plenty of applications such as, paints and varnishes for finishing coats, solid tires, furniture, automobile seats, construction sealants, and adhesives.

Polyurethanes are carbamic acid esters. The urethane functional group is produced by the reaction of an isocyanate functional group and an alcohol functional group:

$$\underset{\text{isocyanate}}{O{=}C{=}N{-}R'} + \underset{\text{alcohol}}{R{-}OH} \rightarrow \underset{\text{urethane}}{R{-}O{-}CO{-}NH{-}R'}$$

The polymer, however, is produced by the polyaddition of a polyisocyanate and a polyol and most of the time in the presence of a catalyst and other additives:

Correspondence to: S. Farzaneh (Sedigheh.farzaneh@ensam.eu).

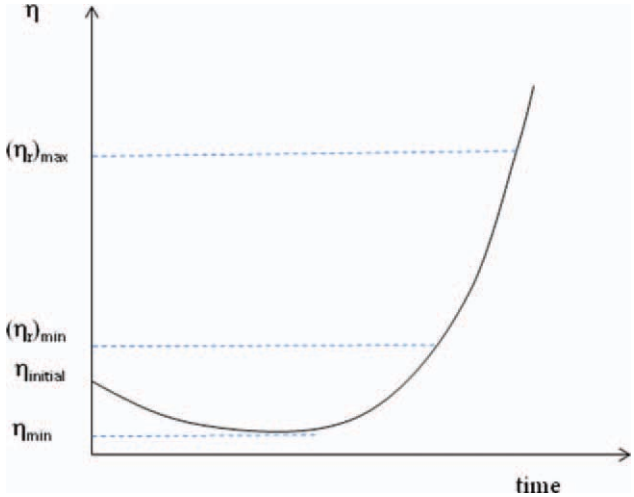

Figure 1 Evolution of viscosity during reactive rotational molding. [Color figure can be viewed in the online issue, which is available at wileyonlinelibrary.com.]

$$\underset{\text{Polyisocyanate}}{R^1{-}N{=}C{=}O} + \underset{\text{polyol}}{R^2{-}OH} \rightarrow \underset{\text{PU polymer}}{R^1{-}NH{-}CO{-}O{-}R^2}$$

The polymerization or the crosslinking of polyurethanes is an exothermic reaction. Because the isocyanate functional group is very reactive to any molecule containing active hydrogen, secondary reactions also take place. The main secondary reactions are described below[6,7]:

Secondary reaction with water:

$$2H{-}OH + \underset{\text{di-isocyanate}}{OCN{-}R{-}NCO} \rightarrow \underset{\text{di-amine}}{H_2N{-}R{-}NH_2} + 2\,CO_2$$

The isocyanate functional group reacts with water, producing at first a very unstable carbamic acid which then breaks down into a diamine and carbon dioxide.

Secondary reaction with diamine:

$$\underset{\text{di-amine}}{H_2N{-}R'{-}NH_2} + \underset{\text{di-isocyanate}}{OCN{-}R{-}NCO} \rightarrow \underset{\text{urea functional group}}{H_2N{-}R'{-}NH{-}CO{-}NH{-}R{-}NCO}$$

The amine produced in first reaction reacts with another isocyanate group to produce a urea functional group.

Nevertheless to simplify the kinetic study only the main reaction is considered in the calculus, that is:

$$O{=}C{=}N{-}R' + R{-}OH \rightarrow R{-}O{-}CO{-}NH{-}R'$$

$$\frac{d[R'NCO]}{dt} = \frac{d[ROH]}{dt} = -\frac{dc}{dt} = -k[ROH]\cdot[R'NCO] \quad (1)$$

$$\text{At } t = 0;\quad [R'NCO] = [R'NCO]_0 = a,$$
$$[ROH] = [ROH]_0 = b \text{ and } [PU] = 0$$
$$\text{At } t = t;\quad [PU] = c,$$
$$[R'NCO] = [R'NCO]_0 - c \text{ and}$$
$$[ROH] = [ROH]_0 - c$$

The concentration rate of PU then is given by the following equation:

$$\frac{dc}{dt} = k(a-c)(b-c), \quad (2)$$

where k is the constant of reaction rate.

For stochiometric systems $[R'NCO]_0 = [ROH]_0 = a$ and therefore:

$$\frac{dc}{dt} = k(a-c)^2 \text{ then } \frac{dc}{(a-c)^2} = kdt. \quad (3)$$

The analytical solution of this equation will give us a kinetic model for evolution of PU formation.

Time-temperature-transformation diagram

The TTT diagram illustrates the evolution of the physical properties of a thermoset during crosslinking, that is: critical temperatures, transformations, and physical states.[8–11] For example, for a certain isothermal curing, the gel time or vitrification point can be easily determined with the help of this diagram. Among other applications, the TTT diagram defines the manufacturing conditions of a thermoset. In order to be able to interpret a TTT diagram, several concepts must be defined:

- Vitrification is the reversible transformation of a viscoelastic gel or a viscous liquid into a glassy gel-solid. This phenomenon occurs when the material's glass transition temperature, T_g, equals the curing temperature, T_{iso}. When vitrified, the polymer's molecular chain mobility is strongly reduced; the reaction then becomes diffusion controlled.
- Gelation is an irreversible transformation of a viscous liquid into a visco-elastic gel (Fig. 2). During gelation the material's viscosity boosts due to the build-up of an infinite and insoluble network. After gelation, the material continues crosslinking but further shaping is impossible.

The gel point corresponds to the formation of a tri-dimensional gel network. The conversion ratio at gel point, x_{gel}, depends on the functionality, the stoichiometric ratio and the reactivity of the chemical groups involved. The gel point of two monomers (A and B) with iso-reactive functional groups can be calculated by the Macosko-Miller formula:

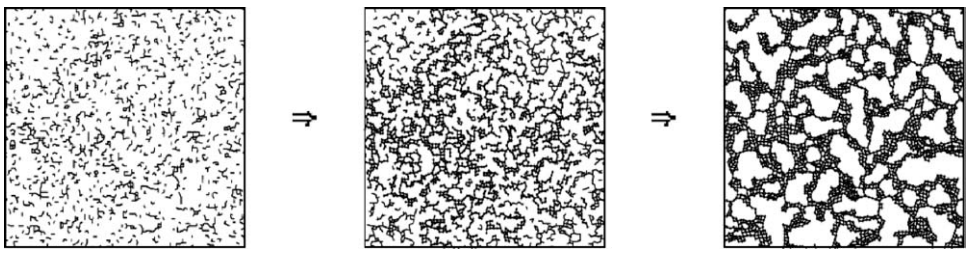

Figure 2 Different steps of gel formation during crosslinking.

$$x_{\text{gel}} = \frac{1}{\left[r\left(1-f_{w,A}\right)\left(1-f_{w,B}\right)\right]^{0,5}} \tag{4}$$

r: stoichiometric ratio; $f_{w,A}$: average functionality of A; $f_{w,B}$: average functionality of B.

Different aspects related to the processing of thermosets may be illustrated by TTT diagram Figure 3. In this diagram:

- The gelation curve can be plotted by the results of rheometrique isothermal tests. The time of gelation in function of the temperature is often modelled by the Arrhenius law.
- The curve of vitrification can be plotted by combination of the results of chemical kinetic model (x in function of time) and the model proposed for the T_g evolution versus conversion ratio, x.
- Thermal stability (degradation boundary) can be determined by the results of gravimetric isothermal analysis (TGA). By this analysis, one may determine the time for 5% of mass loss.

The following critical temperatures are also defined in a TTT diagram:

T_{g0}: the system's initial glass transition temperature.

$T_{g(\text{gel})}$: temperature at which gelation and vitrification are simultaneous.

$T_{g\infty}$: the glass transition temperature of a 100% cured system.

A thermoset suffers different transformations depending on the curing temperature (T_{iso}):

If $T_{\text{iso}} < T_{g0}$, the components don't react together and the rate of the crosslinking reaction is considered negligible.

If $T_{g0} < T_{\text{iso}} < T_{g(\text{gel})}$, the system vitrifies before gelifying, stopping then the crosslinking reaction.

If $T_{g(\text{gel})} < T_{\text{iso}} < T_{g\infty}$, the system gelifies before vitrifying.

$T_{\text{iso}} >> T_{g\infty}$, the thermoset risks degradation.

EXPERIMENTAL

Materials

The polyurethane under study is the system named AT/FPG and provided by Raigi Company. It is a high rate reactive system composed of the stoichiometric mixture ($r = 1$) of the isocyanate, FPG ($f_{\text{w,FPG}} = 2.7$), and the polyol, AT ($f_{\text{w,AT}} = 3$). The weight ratio of isocyanate to polyol is 3 : 2. According to the Macosko-Miller formula, the theoretical conversion ratio at gel point for this system is $x_{\text{gel}} = 0.54$.

ANALYTICAL TECHNIQUES

Thermal analysis

The polymerization of the polyurethane system is studied by means of a differential scanning calorimeter DSC-Q10 from TA Instruments. The calorimeter is calibrated in enthalpy and temperature scales by using a high purity indium sample. Two different methods have been used.

In the first method, the DSC non-isothermal tests have been performed on the isothermally cured samples at different time of curing. These tests, let to study the time evolution of the crosslinking reaction, that is: $x_{\text{DSC}} = f(t)$, by measuring the residual enthalpy, ΔH_{res} at each conversion ratio and then using the formula:

$$\left(x_{\text{DSC}} = 1 - \frac{\Delta H_{\text{res}}}{\Delta H_{\text{tot}}}\right)$$

where ΔH_{tot} is the total enthalpy of crosslinking reactions.

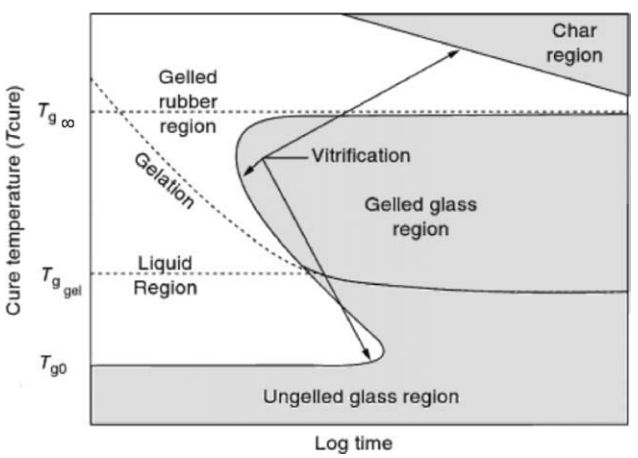

Figure 3 TTT diagram for a reactive system.[12]

TABLE I
The Method Used for the DSC Tests

	Step	Aim
1	Isothermal curing temperature: T_{iso}	Isothermal curing phase.
2	Curing time	
3	Equilibrate at −50°C	Quit cross-linking by vitrifying the sample.
4	Scanning at 5°C min^{-1} up to 200°C	Measurement of T_g and ΔH_{res} of the partially reticulated sample.

The measurement of the glass transition temperature for a given time and conversion ratio: $T_g = f(t)$ and $T_g = f(x_{DSC})$.

DSC tests are performed under inert atmosphere (nitrogen). The temperature rate was 5° min^{-1}. The samples have a mass of ~ 15 mg and are placed in hermetic aluminium capsules. Isothermal curing was performed at 25, 30, 35, 40, and 45°C. This method is described in Table I.

In the second method, isothermal DSC test has been performed on one non-cured sample. By integrating the exothermic curve, the evolution of conversion ratio has been followed during the time, using the following equation:

$$x_{DSC} = \frac{\Delta H_t}{\Delta H_{tot}}$$

where ΔH_t is the exothermic enthalpy at a given time of crosslinking and ΔH_{tot} is the total enthalpy of isothermal crosslinking.

Rheological analysis

Rheological properties are measured using an Ares Rheometer from TA Instruments equipped with 25-mm diameter parallel plates. The aim of these tests is to determine the system's gel point at different temperatures (25, 30, 35, 40, and 45°C). To do so, the material's rheological properties are measured in multifrequency mode. Measurements are taken each 8 seconds and the gap between parallel plates is between 0.5 and 1 mm wide.

Infrared analysis

Infrared analyses are carried out, using Bruker IFS28 spectrophotometer, equipped with a Globar source, KBr beam splitter and DTGS detector, in order to study the real time evolution of the crosslinking reaction. All spectra were collected in the near infra red domain (4000–400 cm^{-1}) at a 4 cm^{-1} resolution and 32 scans per sample. For thermal control, a temperature controller is used (Specac). The reactive mixture is injected with a syringe in the cell (Quartz with 2 mm pathlength) when the controller showed the programmed temperature.

The disappearance of the isocyanate group and the formation of the PU group are monitored every minute for the first half hour of reaction and then every hour for a total of 15 h.

To determine the PU conversion ratio, the same cell is used for all experiments, therefore we applied the simple equation:

$$x = 1 - \frac{A_t}{A_0}$$

where $\frac{A_t}{A_0}$ is the ratio of actual area of peak with respect to initial one.

RESULTS AND DISCUSSION

Thermal analysis

The DSC test results are represented in thermograms such as the one illustrated in Figure 4. The first inflexion point symbolizes the glass transition temperature (T_g) of the partially crosslinked sample. The residual enthalpy (ΔH_{res}) is calculated by integrating the exothermic area of the curve.

As an example, Figure 5 illustrates the superposition of the nonisothermal DSC thermograms obtained after the different isothermal curing time at 30°C (first method).

Figure 5 shows the glass transition temperature increases with the curing time. Nevertheless, the

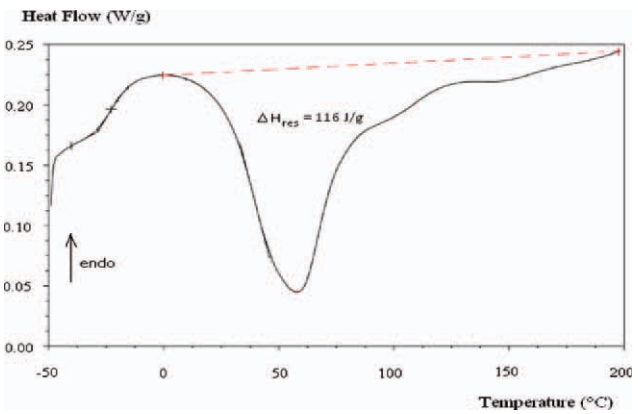

Figure 4 AT- FPG thermogram corresponding to a 10 min isothermal crosslinking at 25°C. [Color figure can be viewed in the online issue, which is available at wileyonlinelibrary.com.]

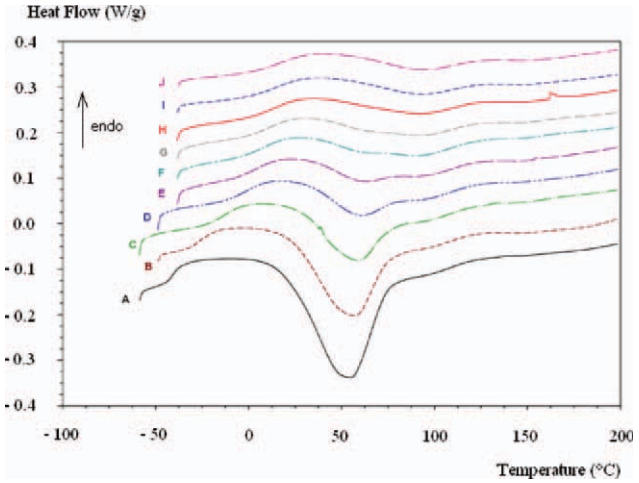

Figure 5 DSC thermograms of cured samples of AT-FPG system at 30°C. Curing time for different samples: 0 min (A), 5 min (B), 10 (C), 20 min (D), 30 min (E), 40 min (F), 50 min (G), 70 min (H), 90 min (I), and 120 min (J). [Color figure can be viewed in the online issue, which is available at wileyonlinelibrary.com.]

residual enthalpy decreases and thus the conversion ratio, x_{DSC} increases with time. The same happens at all the studied temperatures.

The quantitative test results performed at 30°C are presented in Table II. With these results, the relations $x = f(t)$ can be drawn as shown in Figure 6.

These results then are compared with the results obtained from one sample isothermal curing using running integral method (second method). One can see a good agreement between two methods.

This evolution has direct effect on T_g. Indeed T_g of the system increases vs. time (Fig. 7) and conversion ratio (Fig. 8).

The evolution of T_g versus the conversion ratio can be presented by Di Benedetto modified equation[13]:

TABLE II
AT-FPG Thermal Analysis Results at 30°C

Isothermal time (min)	Glass transition temperature, T_g (°C)	Enthalpy, ΔH (J g^{-1})	Conversion rate x_{DSC}
0	−45	178.2	0
5	−18	131.4	0.263
10	−12	90.7	0.491
20	−5	68.8	0.614
30	2	54.3	0.695
40	7	45.4	0.745
50	9	41.0	0.770
70	11	36.0	0.798
90	14	35.0	0.803
120	17	33.7	0.811
180	20	27.7	0.845
240	25	22.2	0.875
340	27	21.5	0.880
540	31	20.6	0.884

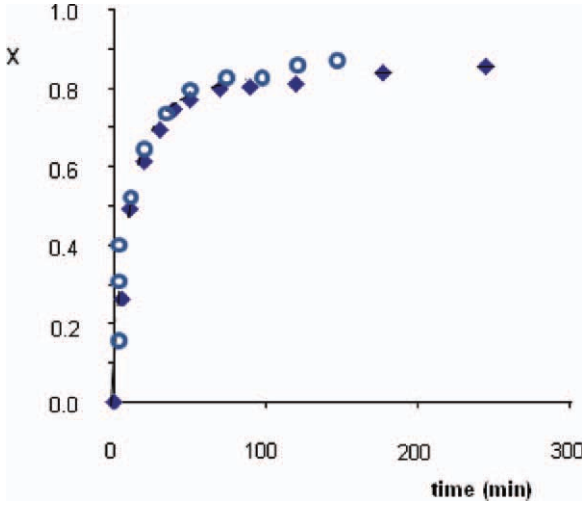

Figure 6 Time evolution of the conversion ratio of AT-FPG at 30°C, obtained by two methods. 1st method (◆), 2nd method (○). [Color figure can be viewed in the online issue, which is available at wileyonlinelibrary.com.]

$$T_g = T_{g0} + \frac{\lambda(T_{g\infty} - T_{g0})}{1 - (1-\lambda)x}, \tag{5}$$

where $\lambda = \frac{\Delta C_p^{\infty}}{\Delta C_p^0}$

ΔC_p^0 = heat capacity of initial system

ΔC_p^{∞} = heat capacity of 100% cured system

This equation can be converted to a linear equation to use linear regression method for modeling:

$$\frac{T_{g\infty} - T_{g0}}{T_g - T_{g0}} = \frac{1}{\lambda} - \frac{1-\lambda}{\lambda}x. \tag{6}$$

Using the value of Table II, $Y = \frac{T_{g\infty} - T_{g0}}{T_g - T_{g0}}$ has been plotted versus conversion ratio, x.

In the case of the reactive system under study $T_{g\infty} = 45$°C and $T_{g0} = -45$°C.

The linearity of this plot with a correlation coefficient of $R^2 = 0.993$ shows that Di Benedetto equation explain well the evolution of $T_g = f(x)$.

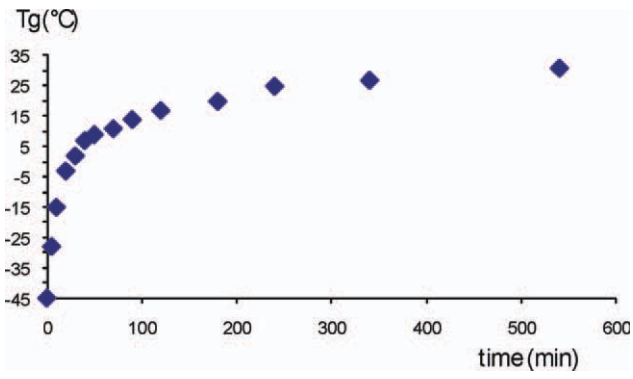

Figure 7 Time evolution of the glass transition temperature of AT-FPG at 30°C. [Color figure can be viewed in the online issue, which is available at wileyonlinelibrary.com.]

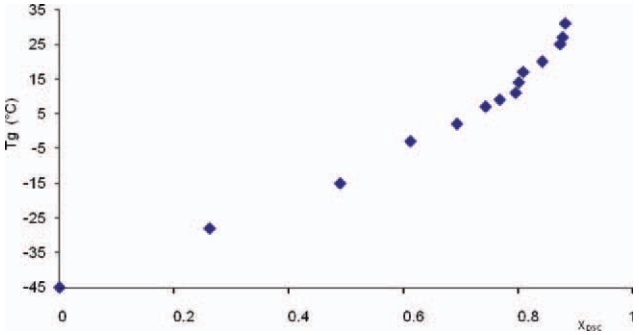

Figure 8 The glass transition temperature of AT-FPG function of conversion ratio at 30°C. [Color figure can be viewed in the online issue, which is available at wileyonlinelibrary.com.]

One may determine the value of λ equal to 0.23. This value is close to the value obtained by DSC test for which $\lambda = \frac{\Delta C_p^{\infty}}{\Delta C_p^{0}}$.

Rheological analysis

The gel point can be defined by three different rheological criteria. A thermoset reaches its gel point when: viscosity (η) tends to infinity, the elastic modulus equals the loss modulus ($G' = G''$), the loss factor (tan δ) is constant at all frequencies.[14]

Figure 9 shows the time evolution of viscosity at different temperatures and frequencies. The system's gel time decreases with temperature, that is, gelation becomes faster as temperature increases.

Figure 10 indicates as an example the evolution of the loss factor (tan δ) measured at four different frequencies (0.25, 1, 2, and 5 Hz harmonics) at 35°C. According to the third criteria, for a given temperature, the gel point is attained at the instant when the loss factor values at all frequencies coincide.

Table III presents the material's gel times at the studied temperatures:

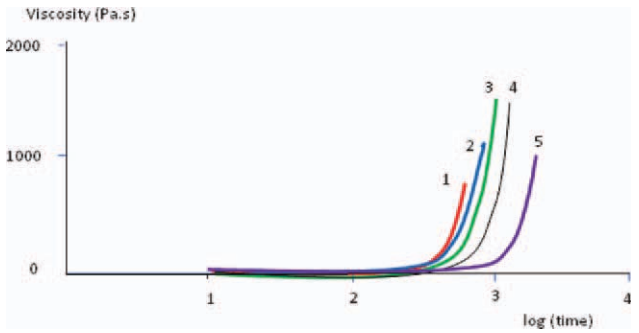

Figure 9 Time evolution of AT-FPG's viscosity at different temperatures and frequencies. (1) 45°C, (2) 40°C, (3) 35°C, (4) 30°C, (5) 25°C. [Color figure can be viewed in the online issue, which is available at wileyonlinelibrary.com.]

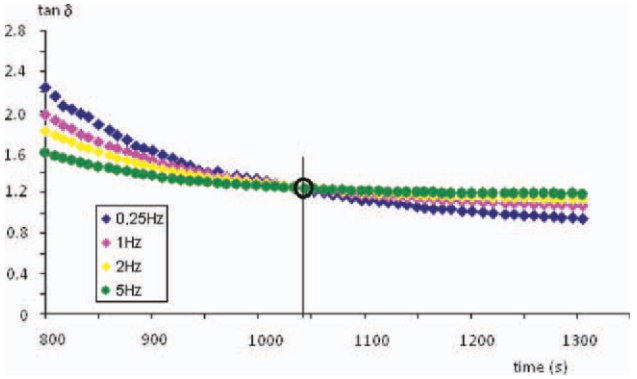

Figure 10 Time evolution of the loss factor at 35°C measured in multi-frequency mode. [Color figure can be viewed in the online issue, which is available at wileyonlinelibrary.com.]

Infrared analysis

Figure 11 illustrates the superposition of the spectrums obtained during the polymerization of the polyurethane system. It is observed that as the crosslinking reaction progresses the isocyanate band (2277 cm^{-1}) decreases, along with the isocyanate functional group concentration.

The graph shown in Figure 12 presents the concentration of the isocyanate and urethane functional groups vs. time.

With the obtained results, the kinetic formula of the crosslinking reaction and formation of polyurethane can be specifically determined for the AT-FPG system:

$$c = [\mathrm{PU}] = \frac{[\mathrm{R'NCO}]_0}{1 + [\mathrm{R'NCO}]_0\, kt} \tag{7}$$

where $[R'\mathrm{NCO}]_0$ is the initial concentration of isocyanate and k is the rate constant of reaction.

This model can be compared by the curve of Figure 13, representing the variation of the concentration of polyurethane.

It seems a good correlation between the theoretical model and experimental results. By this modelling we can obtain the value of rate constant of reaction: $k = 1.15$ L mol^{-1} s^{-1}.

Time-Temperature-Transformation diagram

The glass transition temperature, T_g increases during curing of the mixture of resin and hardener. When

TABLE III
AT-FPG Gel Times

Temperature (°C)	t_{gel} (s)
25	2237
30	1667
35	1044
40	738
45	494

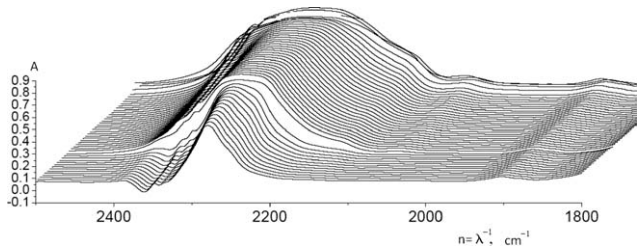

Figure 11 Infrared analyses at 22°C of the polyurethane system AT-FPG.

its value is less than the curing temperature, the molecular mobility is relatively high; the system remains reactive and crosslinking takes place without any major difficulty. When the value of T_g reaches to the curing temperature, the molecular mobility reduces and the reactions will be controlled by diffusion. For higher value of T_g, because of immobility of functional groups crosslinking will stop.

From the results obtained in this work, the TTT diagram is plotted experimentally (Fig. 14). For each isothermal curing temperature, the time takes to gelation (gelation curve) and to vitrification (vitrification curve) are plotted.

The gelation curve follows the Arrhenius rate law:

$$t_{\text{gel}} = A \times \exp\left(\frac{E_a}{R \times T}\right), \tag{8}$$

where E_a is the apparent activation energy, T the absolute temperature of the reaction, R the universal gas constant, and A a constant.

Using the results of the Table III, A and E_a are calculated by linear regression. That is $A = 6.10^{-8}$ s and $E_a = 60.4$ kJ mol^{-1}.

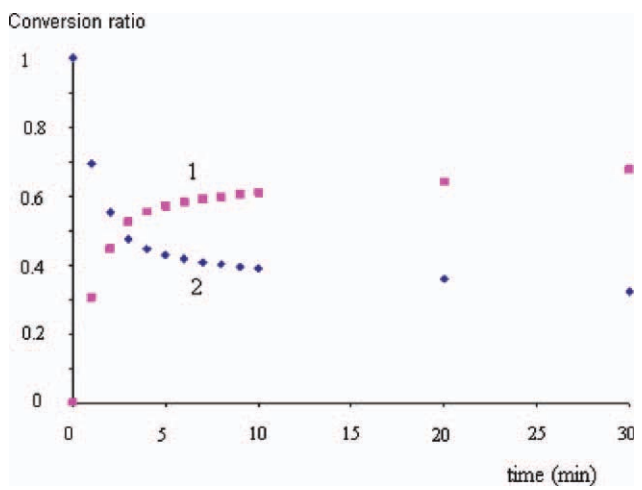

Figure 12 Increase of conversion ratio of polyurethane (1) and decrease of conversion ratio of isocyanate (2) vs. time. [Color figure can be viewed in the online issue, which is available at wileyonlinelibrary.com.]

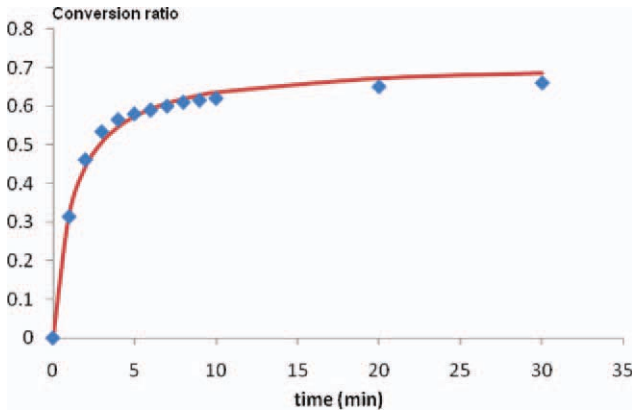

Figure 13 Formation of polyurethane versus time. Experimental curve (◆), theoretical curve (solid line). [Color figure can be viewed in the online issue, which is available at wileyonlinelibrary.com.]

The critical temperatures (T_{g0}, $T_{g\text{-gel}}$, and $T_{g\infty}$) are determined experimentally by thermal analysis.

The TTT diagram can help to determine the AT-FPG manufacturing domain. In the case of reactive rotational molding, the processing is controlled by the variation of viscosity during polymerization. The suitable viscosity interval for rotational molding is limited by a maximum viscosity represented by the gelation curve and minimum viscosity, which depends on the mold's dimensions and rotation speed. The rotational molding domain is also limited by a minimum temperature represented by $T_{g(\text{gel})}$.

CONCLUSION

The polyurethane's crosslinking reaction has been kinetically analyzed. A kinetic model based on a simplified mechanism has been proposed. This model was verified by experimental results obtained by infrared spectrometry. The conversion ratio followed also by differential scanning calorimetric analysis. It has been shown that the evolution of glass

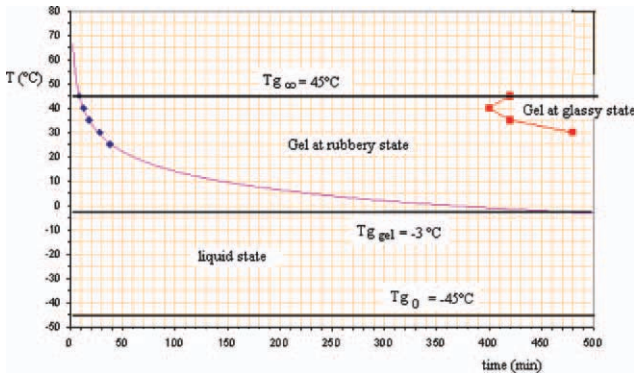

Figure 14 AT-FPG TTT diagram. [Color figure can be viewed in the online issue, which is available at wileyonlinelibrary.com.]

transition temperature corresponds well the Di Benedetto-modified model.

The gelation of the reactive system was studied in isothermal curing conditions. The time evolution of the system's rheological properties has been measured at different frequencies (multifrequency mode). The criteria used to determine the gel point is the instant where the loss factor values at all frequencies become the same. The evolution of gel time as a function of temperature follows an Arrhenius rate law.

The thermal and rheological behaviors of the polyurethane system AT-FPG have been studied for reactive rotational molding time and temperature intervals. The thermal (vitrification curve) and rheological (gelation curve) results are presented in the time-temperature-transformation diagram. The TTT diagram shows the system's optimal conditions for rotational molding.

The authors thank RAIGI Company and CEA (Commissariat à í énergie atomique) for their help and for their active participation in this project.

References

1. Harkin-Jones, E.; Crawford, R. J. In Rotational Molding of Plastics, 2nd ed.; Crawford, R. J., Ed.; RSP Ltd.: Taunton (UK), 1996; 243.
2. Tcharkhtchi, A.; Verdu, J. J Adv Eng Mater 2004, 6, 983.
3. Corrigan, N.; Kakin-Jones, E.; Brown, E.; Coates, P. D.; Crawford, R. J. Plast Rubber Compos 2004, 33, 37.
4. Baker, J. W.; Holdsworth, J. B. J Chem Soc 1947, 26, 713.
5. Dimier, F. Injection de Systèmes Réactifs: Détermination de Lois Cinétiques et Rhéologiques et Modélisation, PhD Report, Mines ParisTech, December, 2003.
6. Thiele, L. Acta Polyerica 1979, 30, 323.
7. Hepburn, C. Polyurethane Elastomers, 2nd ed. Elsevier Applied Science: London, 1991.
8. De Miranda, M. I. G.; Samios, D. Eur Polym J 1997, 33, 325.
9. Mounif, E.; Bellenger, V.; Tcharkhtchi, A. J Appl Polym Sci 2008, 108, 2908.
10. Ennes, J. B.; Gillham, J. K. J Appl Polym Sci 1983, 28, 2567.
11. Nunez, L.; Fraga, F.; Castro, A.; Nunez, M. R.; Villanueva, M. M. Polymer (Guildford), 2001, 42, 3581.
12. Menczel, J. D.; Prime, K. B. Thermal Analysis of Polymer: Fundamentals and Applications; Wiley: New Jersey, 2009; 688.
13. Pascault, J. P.; Williams, R. J. J. J Polym Sci Part B: Polym Phys 1990, 28, 85.
14. Halley, P. J.; Mackay, M. E.; Goerge, G. A. High Perform Polym 1994, 6, 405.